

Structural Analysis Of L-Section With Performance And Strength Of Different Uncertainties Using Simulation With Practical

A.ANBUCHEZIAN , M.VAIRAVEL

Principal & professor , Department of Civil Engineering , AnnaPoorana Engineering College , Sankari Main Road Periya Seeragapadi, Salem, Tamil Nadu 636308.

Associate professor, Department of Civil Engineering , AnnaPoorana Engineering College , Sankari Main Road Periya Seeragapadi, Salem, Tamil Nadu 636308

Abstract

An important problem was identified in the framework of building to resist the whole tectonic loads. And also it identifies the components of structure which gives a potential for certain interruption, capability, transfer the tectonic loading to the array connection in a safe way and finally having adequate strength. The joint of L-section was molded using various rank of concrete and various sizes to reinforce the given connection with various loading. L-section also reduces the height of the one floor to another floor, appropriate connection, economical and technical problems. It also created the latest composite connection which joined the proposed structural system. It was investigated both analytically and experimentally. This paper focuses to consume the appropriate methods to resist earthquake model based on the stiffness, building strength and capacity of elasticity. These methods are used to withstand the building during the heavy earthquake time. The development of L-section was presented the loading process and the capacity or strength of various problems.

Keywords: L-Section, Cyclic load, GFRP mesh, Ductility, Energy absorption, Stiffness.

Introduction

Utility requirement may make it desirable to use openings in the pre-tensioned inverted L-Section. However, introducing an opening into the web of a pre-stressed concrete beam reduces stiffness and leads to more complicated behavior. [1] Therefore, the effect of openings on strength and serviceability

must be considered in the design process. Numerous investigations have been carried out on reinforced concrete section with opening. The pre-stressed beam with web openings has investigated pre-stressed section with web openings. It has been realized that there were scarce published research works on strengthening around web openings with GFRP (Glass Fiber-Reinforced Polymer). [23] As such, this piece of research report focuses on this particular area. Columns are important members of a Reinforced Concrete (RC) structures. Column cross sections can be of different shapes. Out of these, rectangular or square cross sections are very common. Many a time when such cross sections are used, offsets appear at the junction of wall and column, which may not look pleasing from an aesthetic point of view and such offsets can be avoided if L-Section can be substituted for them by providing equivalent concrete area in L-Section having flange thickness or web thickness equal to thickness of wall. Experimental work on T-shaped RC members under uniaxial bending has been scarce. But, design of L-section columns under axial load and biaxial moments based on limit state method of design as per IS 456:1978 has already been done. The optimal design of the critical sections is known only for rectangular sections. [15] For other geometries, research has been made in terms of the biaxial interaction diagrams. These diagrams attempt to make an optimization by a trial and error procedure. The importance of the development of the optimal design of L-Sections is due to the fact that it is currently a frequently used section in common structures. Another relevant aspect is that the methodology used can be extended to other sections and included in the computer codes with minimum programming. [14] The design variables considered in the optimization of the reinforced beam with an L-Section are the steel area and the steel localization, either in the tension or in the compression zones. The equilibrium equations of a reinforced concrete L-Section under Limit State Design are defined by the non-linear behavior of the concrete and the steel. [7][8]

L-section

L-section was used to give required compression place for a separated array, consistency which could be in the range of $\frac{1}{2}$ widths and border width could not exceed four times the network width. An effective width in border could not overlap $\frac{1}{4}$ of the spanning beam for a symmetrical L-beam. The effective width in border could not overreach $\frac{1}{12}$ th span and the consistency of the slab was six times greater than it. [21] An extension of L-section could be modeled to work as an arch design. A reinforcement arch could not overreach five times the consistency of border. It was analyzed as a single reinforced array with the consistency of arch design. It was clearly explained in the figure 1.



Figure 1 Effective L-Section Flange

Effective Flange Width

Stresses are considered to be stable with the array width in the fundamental theory of bending. When the width consistency was large, it does not take its whole share in existing moment in bending. This flange width also has the stress difference. [11] The distribution of stress was replaced by the correct distribution depend on the rules of constant equivalence which is used to simplify the design and analysis of L-section. It was clearly explained in the figure 2.

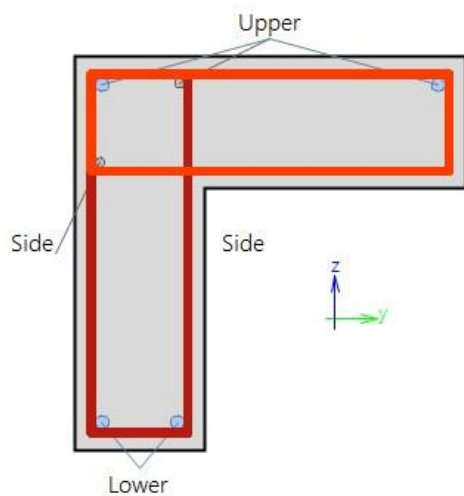


Figure 2 Effective L-Section Flange Widths

An effective consistency of an L-section was explained in the figure 3 according to ACI 8.12.2. It does not overreach the smallest of Width of web plus 16 times slab thickness, b_w+16t , center-to-center spacing of beams and One-fourth the span length of the beam, $L/4$. [9]

Here b_w be the effective flange width of web, t is the slab thickness and L is span of beam. For L-shaped beams, ACI 8.12.3 requires that the effective flange width not to exceed the smallest of

- I. $b_w + L/12$
- II. $b_w + 6t$
- III. $b_w + \text{Half clear distance to the closest beam.}$

For isolated beams in which the T-shape is used to provide a flange for additional compression area, ACI 8.12.4 states that the flange thickness is not to exceed half the web width, $\frac{b_w}{2}$, and the effective flange width b_e not more than four times the web width, $4b_w$. [10]

Descriptive and Methodology:

An important problem was identified in the framework of building to resist the whole tectonic loads. And also it identifies the components of structure which gives a potential for certain interruption, capability, transfer the tectonic loading to the array connection in a safe way and finally having adequate strength. [17] The joint of L-section was molded using various rank of concrete and various sizes to reinforce the given connection with various loading. L-section also reduces the height of the one floor to another floor, appropriate connection, economical and technical problems. The materials and procedures analyzed in this paper and also talks about the physical property of the things. The items used for this research were GFRP mesh, M-sand, coarse aggregate, cement, fly ash, water, fine aggregate, powerful strength and super plasticizer which are discussed in the below section. [16], [19] Figure 3 illustrates the L-section model and the procedures proceed in this research are depicted in fig.4

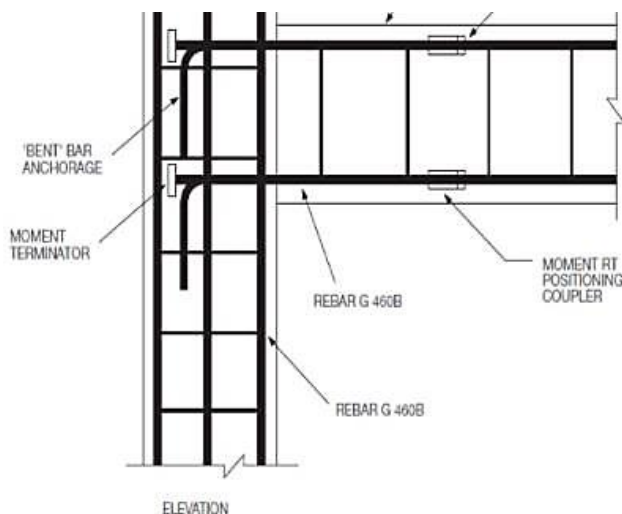


Figure 3. L-section was molded

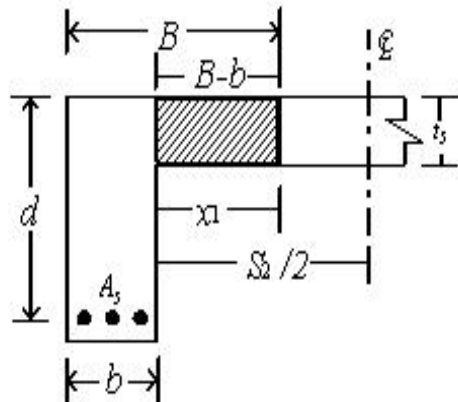


Figure 4. L-section was molded using various rank of concrete

Materials and Methods:

Fibres are the important elements to fortify the composite items in fiber. Fibres possess the large division of volume especially to offer the important segment and overlay in composite material. It is applicable to fortify the fiber based on the filaments introduction, sort, volume and length in the network. GFRP bars are utilized as important reinforcement for the structure. [20] Glass Fiber Reinforced Polymer material broadcasts the direct stability fear strain features which disappointed with very low modules of versatile steel material. It increases stresses on the execution of glass fibre reinforced polymer structures. It needs the energy disappearance by the plastic condition. This type of glass fibre was known as Fibre Glass. This fibre glass was not only light weight material but also vigorous to handle. The crude material was less expensive and less weak. Table 2 and Fig. 6 explain about the property of the glass fibre mesh. [22]

Table 1 Properties of Glass Fiber mesh

S.No	Characteristic of glass fiber mesh	Values
1	Tensile strength(MPa)	3390
2	Compressive Strength (MPa)	1100
3	Density (g/cm ³)	2.59

4	Thermal expansion ($\mu\text{m}/\text{m}.\text{°C}$)	4.67
5	Softening T (°C)	850
6	Poisson`s ratio	0.3

Re Araldite® AW 106/Hardener HV 953 U was used for multiple purpose such as toughness, high quality in sticky like substance, curing in room temperature. It was comfortable to hold some wide materials like plastic which is inflexible, elasticity, pottery, metals, glass and various things which are used for common places. Tab.1 narrates the hard property and fig. 5 explains the hard araldite.Table 2 describes the Araldite AW 106 & Hardener HV 953 U

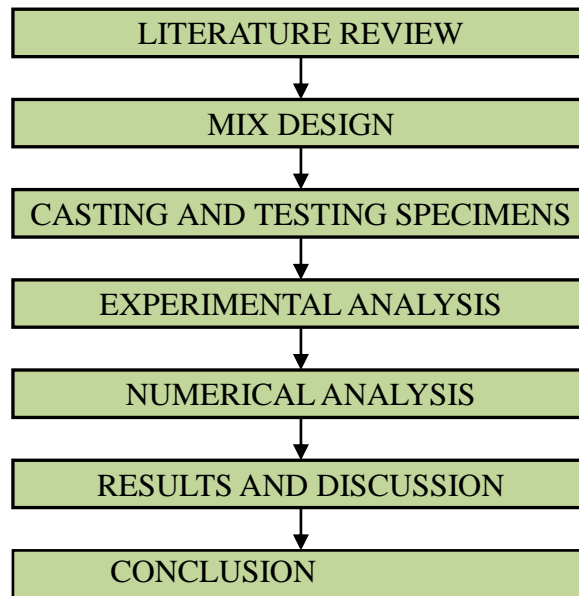


Figure 5. Research Methodology

Table 2 Description of Araldite AW 106 & Hardener HV 953 U

Properties	Araldite® AW 106	Hardener HV 953 U	Mix
Colour (visual)	Neutral	Pale yellow	Pale yellow
Specific gravity	Ca. 1.15	Ca. 0.95	Ca. 1.05
Viscosity at 25 °C	30-50(Pas)	20-35(Pas)	30-45(Pas)

Pot Life(100 gm at 25°C)	-	-	Ca. 100 minutes
Shelf life(2-40°C)	3 years	3 years	-

The concrete ranking was examined in this paper. The concrete used the M25 grade and steel was Iron500 grade. The mixed ratio of concrete was shown in tab. 3

Table 3 Mix Proportion of cement for reinforcement

Cement (kg)/m ³	Fly ash (kg)/m ³	FA (kg)/m ³	CA (kg)/m ³	Water (kg)/m ³	Super Plasticizer (kg)/m ³
265	112	743	1200	190	9.14
1		1.80	3.76	0.454	0.195

Specifications of the sample:

An intersection of column and beam are called L-joints parameters or junction or joint. These are analyzed in this section. The characteristics of L-section depend upon the load process which are identify the factor values of ductility, absorbing energy, maximum worry, variation in strength and displacement. These were examined through analytically and experimentally by the Analysis System software. It was clearly shown in the fig.6



Figure 6 Araldite Hardener

The whole L-connections of column and beam were investigated in this research paper. The 1st illustration CT1 is examined the control of base specimen. [12] It has banished beam of 1.10 meter

length and 1.100m X 1.100 m cross dimension. Beam was joined to a column at the middle point in height. The dimension of the column is 1.100m X 1.100 m. The whole length was 2.0 meter which is splitted into 2 parts, they are upper and lower part. The lower and upper swelling of the beam and the basic longitude steel column develops from high steel tensile.[13] The middle steel of the shaft was 2 bars of 11mm in diameter and secondary one was also 11mm in diameter. The column swelled with 4 bars of 11mm diameter at each and every corner of the cross dimension column. The Glass fibre Reinforced Plastic mesh and L-section was illustrated in the fig. 7. The examined L-section specimen in the frame was shown in the fig.8



Figure 7 Glass Fiber Mesh



Figure 8 L-section specimen in the frame

An external column and beam connection was exposed to assume the static loading of earthquake. Here loads were proceeding at the end form 5KN to 22 KN. If the load was high, then the tensile and compressive force are operated at upper and lower distance of 560 mm from the column. It was loaded under stable compressive at the top and the lower beam was joined to the underground. [4] It represents $0.3f_{ck}$ of the static load in the column. An instrument named reflectometers is used to

analysis the displacement of the examples. The plate of 7mm density was given at the loading point to ignore the local tensions. The examination setup for upward and downward loading was explained in the fig.9 and 10.



Figure 9 Placing of GFRP mesh inside the mould and casting of L section specimen

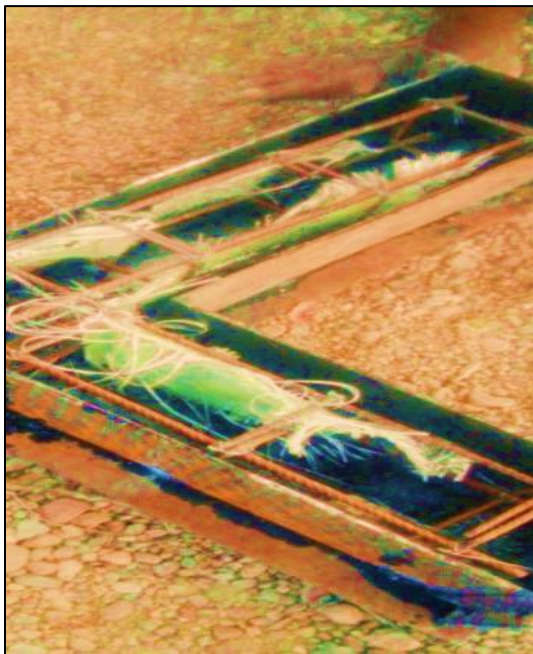


Figure 10 Placing of GFRP mesh inside the mould and casting of L section specimen

EXPERIMENT:

A concrete L-section and HSL section, columns are connected at every ends of the beam. To protect the illustration from the action during the testing time, a wrapped rod was given around the column. The

displacement of illustration was calculated using the instrument of deflectometer. [6] The greatest capacity of loading till 60Kn was calculated by verifying ring. The results of the test were taken experimentally and analytically which are discussed under.

During each process, there is a gradual increment in the level of loading. The logical sequence of load was 4kN, 8kN, 12kN and so on. A measurement of deflection was 0.45mm at the downward load and the upward load was 0.45mm. At the time of downward, the 1st process of load was 5kN and at the time of upward, the 1st process of load was 8kN. The cyclic loading and measurements of deflection for L-section were shown in the figure 11. The maximum measurement of deflection was 6.01mm at the load of 78kN.



Figure 11 Proposed R.C.C T sections

The process of loading and factor of tectonic for I-section without Glass fiber reinforced plastic was shown in the fig. 11. A quantity observation of tectonic was explained detail with its reference of deformation of loading response which was always bilinear. [2][3] The proportion of greatest deformation of a specific process to the deflection may provide a measurement of tectonic displacement. The value of tectonic at the 1st process of loading obtained was 1.45 for reverse and 0.7

for forward. The process of loading and cumulative tectonic factor for L-section without Glass fiber reinforced plastic was shown in the figure 12. The sequences of loading were shown in the fig.13.



Figure 12. Cyclic load testing setup on L-section for downward load



Figure 13 Cyclic load testing setup on L-section for upward load

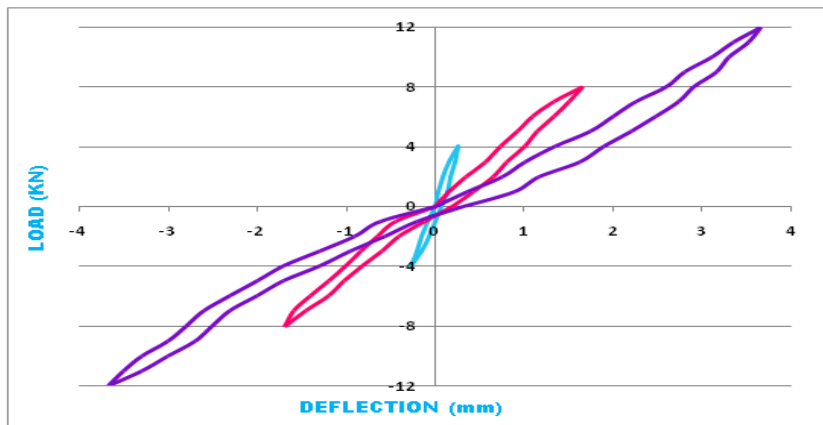


Figure 14 Cyclic loads vs. deflection for L section without GFRP mesh

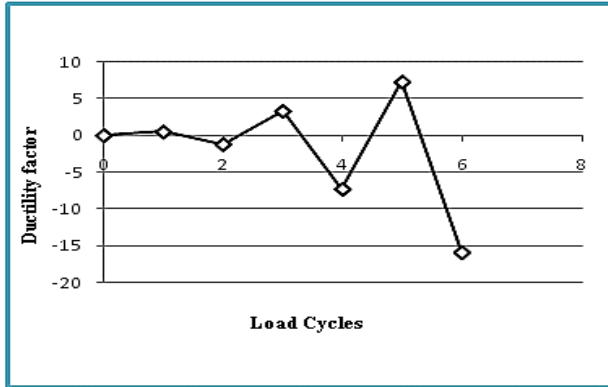


Figure 15 Load Cycles vs. Ductility Factor

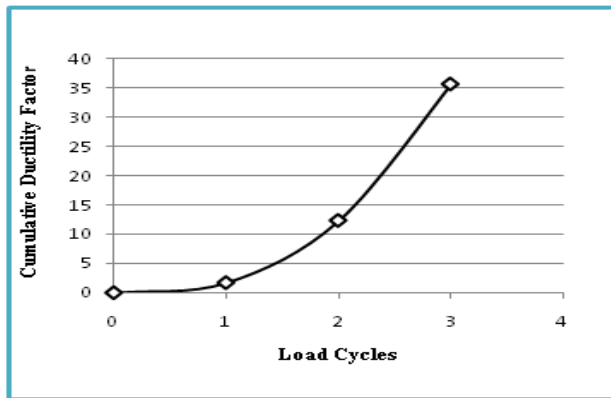


Figure 16 Load Cycles vs. Cumulative Ductility Factor

The difference in strength was shown in the figure.13. The value of strength was analyzed at the 1st process of cycle of 5.45kN/mm and the value of strength was reduced at the increase of load to the greatest of 13kN at the process of loading with the value of 0.78kN/mm. The cyclic process and absorption of energy for reverse and forward with the process for L-section without Glass fiber reinforced plastic was shown in the figure 17 to 20. The capacity of absorption of energy at the cyclic process was measured as the addition of some areas form the deflection of load diagram. The energy absorbed at the 1st process of loading was measured as 0.4kN mm and at the 6th process 4.76kN-mm. Figure 21 and 22 shows the deflection diagram for upward loading on L section.

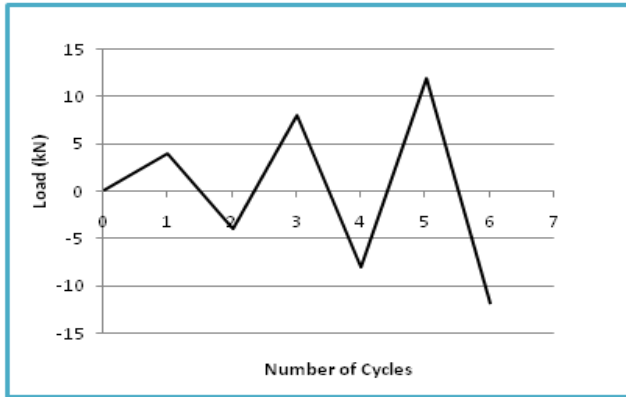


Figure 17 Number of cycles vs. Load

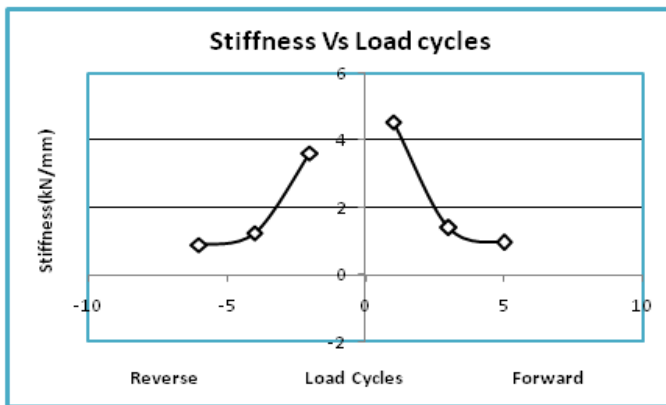


Figure 18 Variation of Stiffness with Load cycles

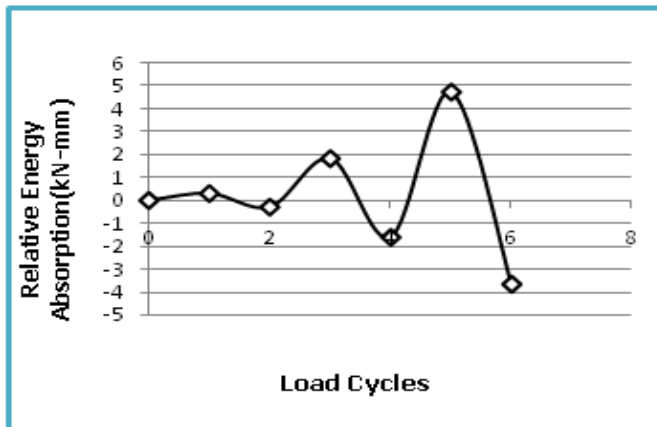


Figure 19 Load cycles vs. Relative Energy Absorption

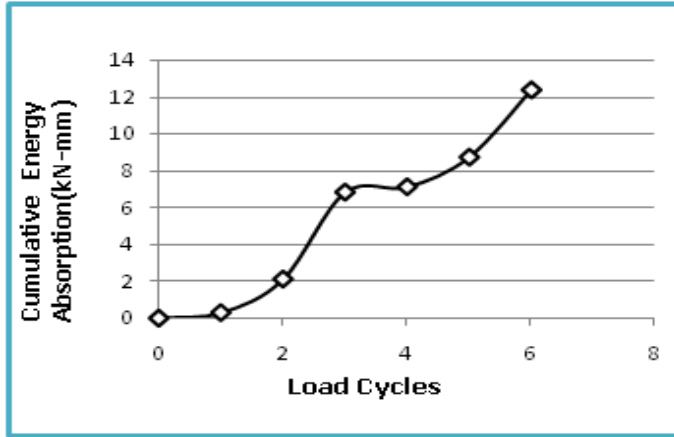


Figure 20 Load cycles vs. Cumulative Energy Absorption

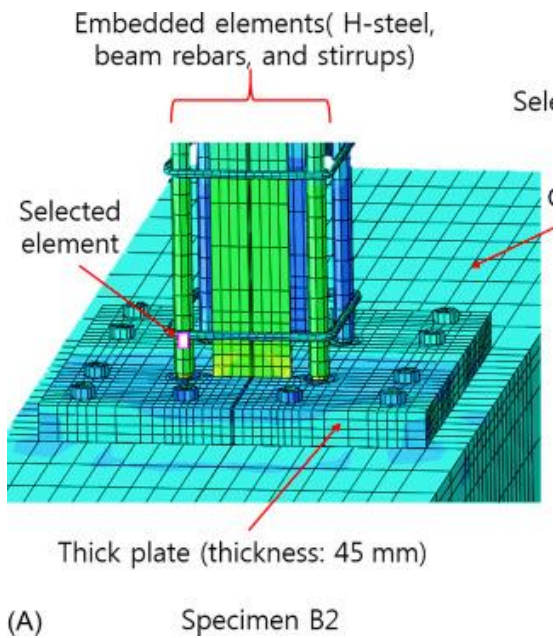


Figure 21 Deflection Diagram for upward loading on L section without GFRP mesh

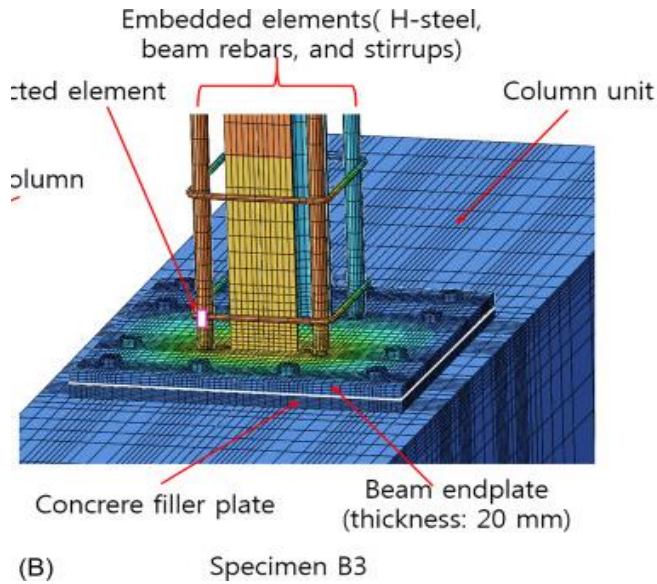


Figure 22 Deflection Diagram for upward loading on L section without GFRP mesh

The cyclic process and the energy absorption for L-section without Glass fiber reinforced plastic were shown in the fig. 23. The capacity of energy absorption was examined by including the capacity of absorption of energy at each process of value that was shown in the tab.4. The absorption of energy by the L-section without Glass fiber reinforced plastic was analyzed as 13.47Knmm at 13kN loading process.

Table 4 Experimental test results for L-Section without GFRP mesh under Cyclic loading

S.No	Cycle No	Max load (kN)	Max deflection (mm)	Ductility factor	Cumulative D.F	Energy Absorption (kN-mm)	Cumulative Energy Absorption (kN-mm)	Stiffness (kN/mm)
Forward Cycle($\Delta y=0.5$ mm)								
1	2	4	0.98	0.90	0.40	0.50	0.50	4.45
2	4	8	1.90	3.98	3.80	1.45	2.12	1.45
3	6	12	3.89	7.30	11.56	4.77	6.84	0.68
Reverse Cycle($\Delta y=0.23$ mm)								
4	3	6	0.87	1.38	12.43	0.30	7.13	3.34
5	6	12	1.98	7.45	19.90	1.63	8.54	1.43

6	9	18	3.90	15.34	35.56	3.65	12.45	0.09
---	---	----	------	-------	-------	------	-------	------

The L-section specimen without Glass fiber reinforced plastic under reverse and forward loading was illustrated in the tab.4. An illustration was attained the value of tectonic as 16.87 at 13kN and also absorption of energy of 5.45kNmm. Simultaneously, the no. of process was increased by tectonic factor, absorption of energy, strength, cumulative absorption of energy and cumulative tectonic factor.

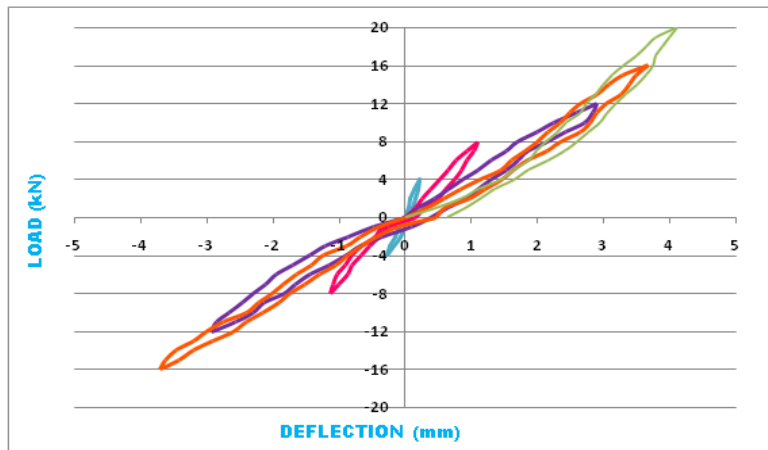


Figure 23 Cyclic loads vs. deflection for L section with GFRP mesh

A diagram of deformation for L-section with Glass Fibre Reinforce Plastic was shown in the fig.23. A maximum loading of 15kN was enforced on the illustration which provides a greatest deviation of 4.98 mm. An equivalent tension for the L-section with Glass fibre reinforced At maximum loading of 15kN was enforced on the illustration which provides a greatest value of 132.89Mpa.

A diagram of deformation for L-section with Glass Fibre Reinforce Plastic at maximum loading of 15kN was enforced on the illustration which provides a greatest deviation of 4.98 mm. An equivalent tension for the L-section with Glass fibre reinforced at maximum loading of 15kN was enforced on the illustration which provides a greatest value of 154.89Mpa.

During each process, there is a gradual increment in the level of loading. The logical sequence of load was 3kN, 6kN, 8kN and so on. A measurement of deflection was 0.25mm at the downward load and the upward load was 0. 29mm. At the time of downward, the 1st process of load was 5kN and at the time of upward, the 1st process of load was 5kN. The cyclic loading and measurements of deflection for L-

section were shown in the figure 24. The maximum measurement of deflection was 5.01mm at the load of 23kN.

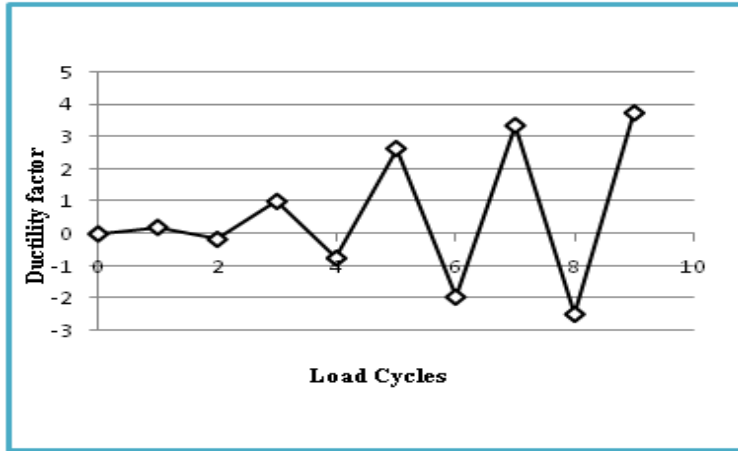


Figure 24 Load Cycles vs. Ductility Factor

The process of loading and tectonic factor for L-section with Glass Fibre Reinforced Plastic was shown in the fig.25. The proportion of greatest deformation process to the deflection may provide a measurement of tectonic displacement. The value of tectonic factor obtained at the 1st process was 0.3 for forward load and for reverse load was 0.18.

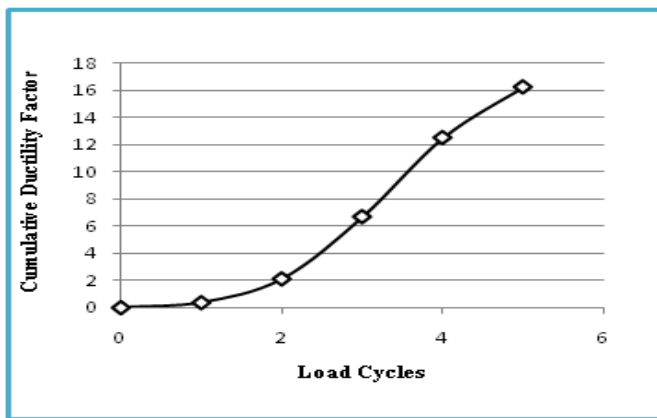


Figure 25. Load Cycles vs. Cumulative Ductility Factor

The process of loading and cumulative tectonic factor for L-section with Glass fibre Reinforced Plastic was shown in the fig.25. the values of tectonic and cumulative tectonic are shown in the tab. 5. The

tectonic cumulative was identified to high from 0.23 at the 1st process of loading to 18.23 at the 9th process of loading. The sequence of loading followed for the investigation was presented in fig. 26.

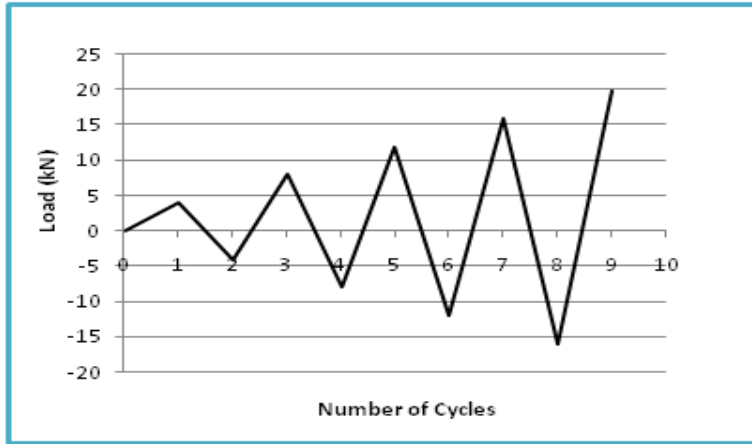


Figure 26 Number of cycles vs. Load

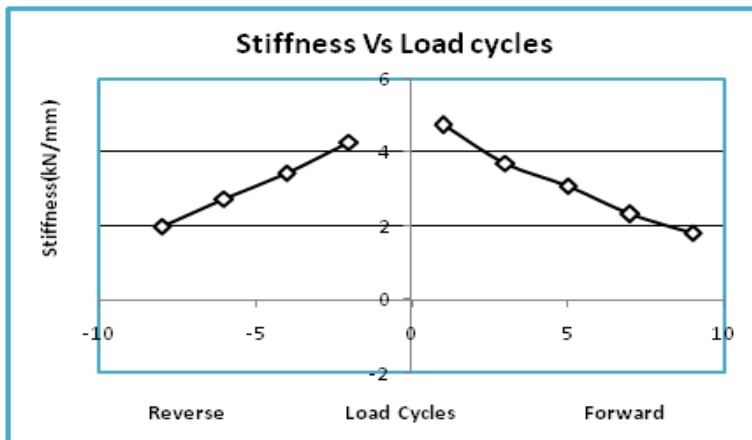


Figure 27 Variation of Stiffness with Load cycles

The difference in strength was shown in the fig. 27 along with the process of loading. The value of strength analyzed at the 1st process of loading with 5.34kN/mm. And the value of strength reduced the loading increment up to the greatest of 25 kN at the process of loading with the value 1.98kN/mm. The process of loading Vs absorption of energy for reverse and forward with the load cycles for L-section with Glass Fiber Reinforced Plastics. It was shown in the figure 26. The absorbed energy at the 1st process of loading was measured as 0.4kN/mm and at the 9th process it was 8.4KN/mm. The absorption of energy and cyclic process for L-section was shown in the figure.26. the capacity of the absorption of

energy was analyzed by including the absorption of energy at the cyclic process and the values are shown in the tab.5

Table 5 Experimental test results for L-Section with GFRP mesh under Cyclic Loading

S.No	Cycle No	Max load (kN)	Max deflection (mm)	Ductility factor	Cumulative D.F	Energy Absorption (kN-mm)	Cumulative Energy Absorption (kN-mm)	Stiffness (kN/mm)
Forward Cycle($\Delta y=1.1$ mm)								
1	2	4	0.23	0.34	0.78	0.34	0.09	4.98
2	4	8	1.14	1.34	1.56	1.90	1.23	3.56
3	6	12	2.91	2.45	3.09	4.09	6.45	3.27
4	8	16	3.45	3.78	7.09	5.98	11.09	2.02
5	10	20	4.13	3.90	10.98	7.56	19.23	1.09
Reverse Cycle($\Delta y=1.5$ mm)								
6	3	6	0.34	0.23	11.29	0.67	19.09	4.22
7	6	12	1.15	0.79	11.24	0.34	20.08	3.56
8	9	18	2.98	1.98	13.67	5.98	25.50	2.09
9	12	24	3.45	2.89	16.90	4.98	30.24	1.23

The results of the section L with Glass Fiber Reinforced Plastic was exhibited under the reverse and forward loads. It was explained in the tab.5. An illustration attains with the greatest quaky factor value of 4.89 at 25kN and the high absorption of energy was 8.45kN mm. Simultaneously, the no. of process increased in greatest loading intersects a greatest deflection by tectonic value, strength, absorption in energy level, absorption of cumulative energy and cumulative tectonic factor. A diagram of deformation for L-section with Glass Fibre Reinforce Plastic was shown in the fig.28. A maximum loading of 27kN was enforced on the illustration which provides a greatest deviation of 5.34 mm. An equivalent tension for the L-section with Glass fibre reinforced Plastic was shown in the fig.29. A maximum loading of 27kN was enforced on the illustration which provides a greatest value of 143.89Mpa.

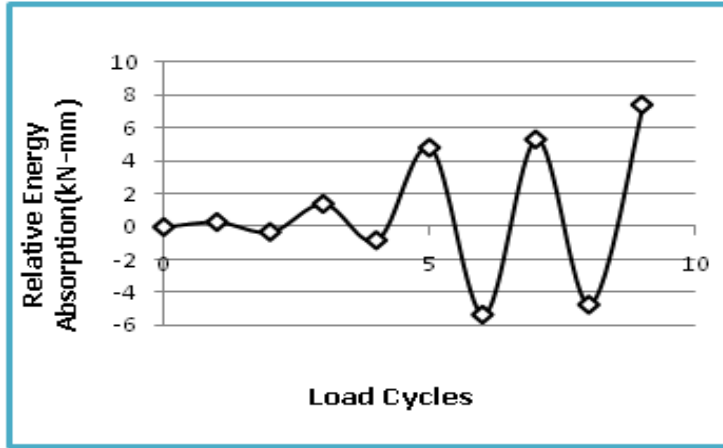


Figure 28 Load cycles vs. Relative Energy Absorption

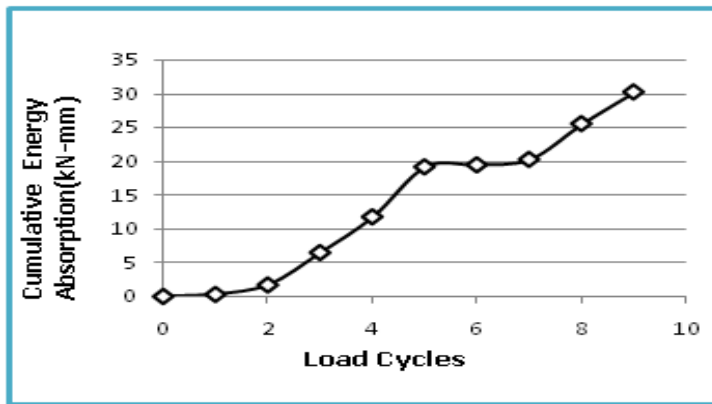


Figure 29 Load cycles vs. Cumulative Energy Absorption

A diagram of deformation for L-section with Glass Fibre Reinforce Plastic was shown in the fig.28. A maximum loading of 25kN was enforced on the illustration which provides a greatest deviation of 5.56 mm. An equivalent tension for the L-section with Glass fibre reinforced Plastic was shown in the fig.29. A maximum loading of 24kN was enforced on the illustration which provides a greatest value of 154.32 Mpa.

Performance Analysis both Experimental and Analytical

In this research, the L-Section specimen was loaded for forward and reverse cycle. The results of the specimens both from experimental and analytical analysis were compared in this portion which includes first crack load and ultimate load of the specimens.

First Crack Load and Ultimate Load for L-Section

Table 6 illustrates the first crack load and ultimate load for L-Section. Figure 34 shows the L-Section results between first crack load and ultimate load. After the specimen was placed in the loading frame and application of load started to the 1st crack was observed at the load of 7kN for conventional concrete and 12kN for GFRP mesh concrete, which shows that there will be an increase in the load resistance by placing GFRP mesh. Also, the ultimate load for conventional concrete was observed as 12kN and for GFRP mesh concrete as 20kN. Thus, the ultimate load increased by 40% in GFRP mesh concrete compared to conventional concrete frame.

Table 6 L-section specimens test results

S.No	Parameters	Conventional Concrete (kN)	GFRP Mesh Concrete (kN)
1.	First Crack load	7	12
2.	Ultimate load	12	20

6.2 Comparison of Results for L-Section Specimens

The results of L-Section for both experimental and analytical examination were compared and found to be similar. The maximum load of conventional concrete was found to be 12kN with the deflection of 3.67mm for experimental which is similar to the analytical value of 12kN load with the deflection of 3.90 mm. Table 7 and Figure 31 shows the load vs. deflection results for each increment of load in L-Section with and without GFRP mesh on experimental as well as analytical analyses. Figure 30 shows the comparison chart for L-section specimens.

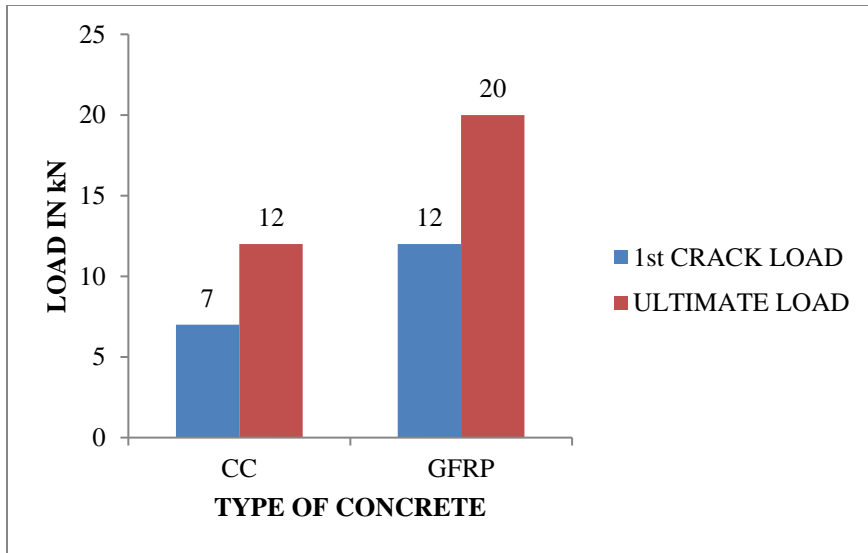


Figure 30 Comparison chart for L-section specimens

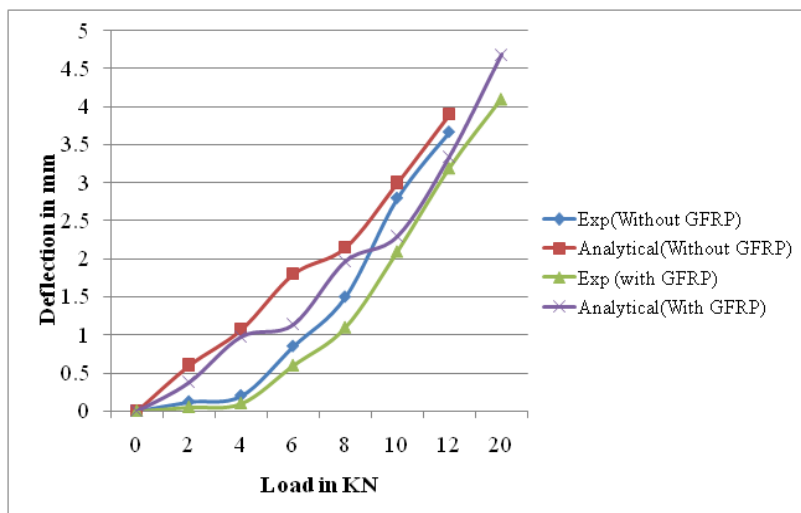


Figure 31 Load vs. Deflection for each increment of load

Table 7 L-section – Test results both experimental and analytical

Load (kN)	Experiment (Without GFRP) (mm)	Analytical (Without GFRP) (mm)	Experiment (With GFRP) (mm)	Analytical (With GFRP) (mm)
0	0	0	0	0
2	0.17	0.60	0.05	0.38

4	0.20	1.07	0.10	0.98
6	0.85	1.80	0.60	1.14
8	1.50	2.15	1.10	1.97
10	2.80	3.00	2.10	2.30
12	3.67	3.90	3.20	3.35
20	-	-	4.11	4.69

Similarly, the maximum load of GFRP mesh concrete was found to be 20kN with the deflection of 4.11mm for experimental which is also similar to the analytical value of 20kN with the deflection of 4.69mm.

Conclusion

An intersection of beam and column and analysis for Glass Fiber Reinforce Plastic are investigated by using Analysis System software 15 through analytically and under the loading process by experimentally. The illustrations are developed as Indian Standard of M25 grade. The specimens are cured and examined with the loading structure process and machine of compression. It also verified that glass fiber reinforce plastic reinforced and play an important role than the consistent loads. Different factors cause the failure in connection under various loading process which are judged using the GFRP in column and beam connection. The external connection of beam and column were examined with various parameters such as strength, maximum stress and deflection. This research was organized to examine the stiff behavior of concrete with Glass Fiber Reinforced Plastic in the L-section. The mixed model of concrete was finished of RM25 grade. The process of the framework of L-section for downward and upward was developed analytically through Analysis System Software packages. The use of Glass Fiber Reinforce Plastic in the consistent concrete ends in an important encouragement in 1st process of loading. Without Glass Fiber Reinforced Plastic of L-section provides a greatest deflection of 4.34mm at 14kN and also gives a greatest deflection of 5.23mm at 25kN loading process. And finally it was analyzed the result from the various examination which accepts with the experiment observation.

REFERENCES

1. Said, Aly M., and Moncef L. Nehdi. "Behaviour of beam-column joints cast using self-consolidating concrete under reversed cyclic loading." 13th World Conference on Earthquake Engineering, Vancouver, Canada. 2004.
2. Alaei, Pooya, and Bing Li. "High-strength concrete exterior beam-column joints with high-yield strength steel reinforcements." *Engineering Structures* 145 (2017): 305-321.
3. Beres, Attila, et al. "Implications of experiments on the seismic behavior of gravity load designed RC beam-to-column connections." *Earthquake Spectra* 12.2 (1996): 185-198.
4. Khene, Ahmed, N. Chikh, and Habib Abdelhak Mesbah. "Numerical modeling of reinforced concrete beams strengthened by NSM-CFRP technique." *Proc. Third International Conference on Architecture, Structure and Civil Engineering*, London, UK. 2016.
5. Bindhu, K. R., Sukumar, P. M., & Jaya, K. P. (2009). Performance of exterior beam-column joints under seismic type loading. *ISCT Journal of Earthquake Technology*, 46(2), 47-64.
6. Celik, Ozan Cem, and Bruce R. Ellingwood. "Modeling beam-column joints in fragility assessment of gravity load designed reinforced concrete frames." *Journal of Earthquake Engineering* 12.3 (2008): 357-381.
7. Choi, Han T., Jeffrey S. West, and Khaled A. Soudki. "Effect of partial unbonding on prestressed near-surface-mounted CFRP-strengthened concrete T-beams." *Journal of Composites for Construction* 15.1 (2011): 93-102.
8. Dessouki, Abdelrahim Khalil, Ahmed Hassan Youssef, and Mohamed Mostafa Ibrahim. "Behavior of I-beam bolted extended end-plate moment connections." *Ain Shams Engineering Journal* 4.4 (2013): 685-699.
9. Sakar, Gokhan, and Omer Zafer Alku. "Strengthening of RC T-Section Beams Subjected to Cyclic Load Using CFRP Sheets." *Advanced Composites Letters* 17.6 (2008): 096369350801700603.
10. Jeon, J. S., et al. "Comparison of fragility curves for an older RC frame with column and beam-column joint shear models." 11th International Conference on Structural Safety and Reliability, ICOSSAR. Vol. 2013. 2013.
11. Kaliluthin, A. K., S. Kothandaraman, and TS Suhail Ahamed. "A review on behavior of reinforced concrete beam-column joint." *International Journal of Innovative Research in Science, Engineering and Technology* 3.4 (2014): 11299-11312.
12. Kane Krutika R & Samarth Gauri V (2017), 'Study of Behavior & Strengthening of Beam-Column Joint', *International Journal on Recent and Innovation Trends in Computing and Communication*, ISSN: 2321-8169, vol. 5, no. 4.

13. Kim, Jaehong, James M. LaFave, and J. Song. "Joint shear behaviour of reinforced concrete beam–column connections." *Magazine of concrete research* 61.2 (2009): 119-132.
14. Li, Bing, and Sudhakar A. Kulkarni. "Seismic behavior of reinforced concrete exterior wide beam-column joints." *Journal of structural engineering* 136.1 (2010): 26-36.
15. LaFave, James M., and Jae-Hong Kim. "Joint shear behavior prediction for RC beam-column connections." *International Journal of Concrete Structures and Materials* 5.1 (2011): 57-64.
16. Massone, Leonardo M., and Gonzalo N. Orrego. "Analytical model for shear strength estimation of reinforced concrete beam-column joints." *Engineering Structures* 173 (2018): 681-692.
17. Mahmoud, Mohamed H., et al. "Strengthening of defected beam–column joints using CFRP." *Journal of advanced research* 5.1 (2014): 67-77.
18. Pamin, Jerzy. "Computational modelling of localized deformations with regularized continuum models." *Mechanics and Control* 30.1 (2011).
19. Park, Sangjoon, and Khalid M. Mosalam. "Experimental investigation of nonductile RC corner beam-column joints with floor slabs." *Journal of Structural Engineering* 139.1 (2013): 1-14.
20. R K, V, KR, B & KV B (2018), 'Probabilistic Model for Shear Strength of RC Interior Beam Column Joints', *Journal of Earthquake Engineering*, pp. 1-20.
21. Rajaram, P., A. Murugesan, and G. S. Thirugnanam. "Experimental Study on behavior of interior RC beam column joints subjected to cyclic loading." *International Journal of Applied Engineering Research* 1.1 (2010): 49.
22. Wan, Yung-Chih, and Kai Hsu. "Shear Strength of RC Jacketed Interior Beam-Column Joints without Horizontal Shear Reinforcement." *ACI Structural Journal* 106.2 (2009).
23. Lu, Xilin, et al. "Seismic behavior of interior RC beam-column joints with additional bars under cyclic loading." *Earthquake and Structures* 3.1 (2012): 37-57.